

# Magnetic and structural study of mechanochemical reactions in the Al-Fe<sub>3</sub>O<sub>4</sub> system

P. M. BOTTA

*Instituto de Investigaciones en Ciencia y Tecnología de Materiales (INTEMA), UNMdP-CONICET, J.B. Justo 4302 B7608FDQ Mar del Plata, Argentina*

P. G. BERCOFF\*

*Facultad de Matemática, Astronomía y Física (FAMAF), UNC, H. de la Torre y M. Allende, Ciudad Universitaria (5000) Córdoba, Argentina  
E-mail: bercoff@mail.famaf.unc.edu.ar*

E. F. AGLIETTI

*Centro de Tecnología de Recursos Minerales y Cerámica (CETMIC) UNLP-CIC-CONICET, Cno. P. Centenario y 506 (1897) M.B. Gonnet, Argentina*

H. R. BERTORELLO

*Facultad de Matemática, Astronomía y Física (FAMAF), UNC, H. de la Torre y M. Allende, Ciudad Universitaria (5000) Córdoba, Argentina*

J. M. PORTO LÓPEZ

*Instituto de Investigaciones en Ciencia y Tecnología de Materiales (INTEMA), UNMdP-CONICET, J.B. Justo 4302 B7608FDQ Mar del Plata, Argentina*

The solid state reaction between Al and Fe<sub>3</sub>O<sub>4</sub> (magnetite) using mechanochemical activation of powder mixtures under Ar atmosphere is studied. The phase evolution during the reaction is analyzed by X-ray diffraction (XRD), vibrating sample magnetometry (VSM), differential thermal analysis (DTA) and scanning electron microscopy (SEM). At 37 minutes of high-energy ball-milling the disappearance of reactive phases and the production of  $\alpha$ -Fe, FeAl<sub>2</sub>O<sub>4</sub> and  $\alpha$ -Al<sub>2</sub>O<sub>3</sub> is observed, together with significant changes in the magnetic behavior of the system. The composition and properties of samples heated up to 1200°C are also investigated. The behavior of the saturation magnetization  $M_s$  is interpreted on the basis of the formation of a variable composition spinel phase Fe [Al<sub>x</sub> Fe<sub>2-x</sub>] O<sub>4</sub> with  $0 \leq x \leq 2$  and a canting effect due to the presence of Al<sup>3+</sup> ions in the spinel structure.

© 2002 Kluwer Academic Publishers

## 1. Introduction

In the last years the mechanochemical activation (or high-energy ball-milling) of crystalline solids has become a widely used tool to synthesize materials [1, 2]. This is due to three fundamental reasons: shortening of reaction times, reduction of the high temperatures usually required for developing solid state reactions, and the possibility to obtain metastable materials with special properties. The great diversity of the mechanochemically prepared materials may be appreciated observing the large amount of bibliography related to this topic. It is possible to find special alloys and intermetallic compounds (FeAl, FeCo) [3, 4], materials for applications at high temperature (borides, nitrides, carbides and silicides) [5–8], ceramics with spinel or perovskite structure for application in electronic

devices [9–11], composite materials (metal-ceramic, ceramic-ceramic, ceramic-polymer) [12–16], etc.

The Al-Fe<sub>3</sub>O<sub>4</sub> system is well known by the highly exothermic reaction that it undergoes when submitted to thermal and/or mechanical treatments, with production of  $\alpha$ -Fe and  $\alpha$ -Al<sub>2</sub>O<sub>3</sub> [17]. If this reaction is mechanochemically induced it is possible to obtain nanocomposites, which are applicable as high-temperature structural materials [18] as well as semi-hard magnetic materials [19]. On the other hand, an appropriate control of the parameters of both processes allows the synthesis of intermediate phases with spinel structure [20], which could find applications in the field of sensors.

In this context, the aim of this contribution is to analyze the reactions between Al and Fe<sub>3</sub>O<sub>4</sub> that produce

\*Author to whom all correspondence should be addressed.

the desired nanostructures as a result of the high-energy ball-milling and subsequent thermal treatment of powder mixtures.

## 2. Experimental

### 2.1. Activation of samples

The starting materials were magnetite (from Sierra Grande, Argentina) containing more than 97.5% of  $\text{Fe}_3\text{O}_4$  and commercial Al powder with a purity of 99.9%. The particle size of both reactants was lower than  $44\ \mu\text{m}$ . Mixtures of these powders were prepared in a Al :  $\text{Fe}_3\text{O}_4$  molar ratio of 2.67.

The mixtures were mechanochemically activated for times up to 75 minutes in hardened Cr-steel milling bowls of 45 ml with 7 balls of the same material in a Fritsch Pulverisette 7 planetary ball mill under Ar atmosphere. The experimental method assured that there was no leaking of oxygen from the outer atmosphere into the vials. They were wrapped up in PE containers which, due to the heat produced by the milling process, were always at a pressure slightly higher than atmospheric. The only possible source of oxygen was some impurity of the used Ar.

The milling media/powder mass ratio was 20 and the speed of rotation was 1500 rpm. The activated samples were named  $S_m$ , where “m” is the milling time, in minutes.

All the samples were heat treated up to  $1200^\circ\text{C}$  under Ar flow (samples  $S_mT$ ). A reddish layer was observed on the top of the samples, which may result from some oxidation to  $\text{Fe}_2\text{O}_3$  due to the residual  $\text{O}_2$  in the chamber.

### 2.2. Sample characterization

The phase composition was analyzed by X-ray diffraction (XRD), using a Philips 1830/00 diffractometer with  $\text{Mo K}\alpha$  radiation ( $\lambda = 0.071073\ \text{nm}$ ). The samples were magnetically characterized in a vibrating sample magnetometer (LakeShore 7300) coupled to an electromagnet, which is able to produce a magnetic field up to 15 kOe. The differential thermal analyses (DTA) were performed in a Shimadzu DTA-50H equipment under flowing Ar, using a heating rate of  $10^\circ\text{C}/\text{min}$  and samples of approximately 40 mg. In order to study the microstructures of the powders a Philips 505 scanning electron microscope (SEM) was used.

## 3. Results and discussion

### 3.1. Effect of mechanochemical treatment

The x-ray diffraction patterns of the series of samples  $S_0$ – $S_{75}$  are shown in Fig. 1. Up to 30 minutes of treatment, the only noticeable effects are the decrease in diffracted intensities and the widening of the peaks (magnetite showed a decrease of about 25% and an average crystallite size of 12 nm for  $S_{30}$ ).

From sample  $S_{37}$ , the presence of hercynite ( $\text{FeAl}_2\text{O}_4$ ),  $\alpha$ -alumina ( $\text{Al}_2\text{O}_3$ ) and  $\alpha$ -Fe is observed together with the disappearance of the pure Al peak. For longer activation times, the alumina and hercynite peaks gradually decrease in intensity, while Fe peaks show a slight increase both in intensity and width (the latter effect probably due to the crystal microstrains

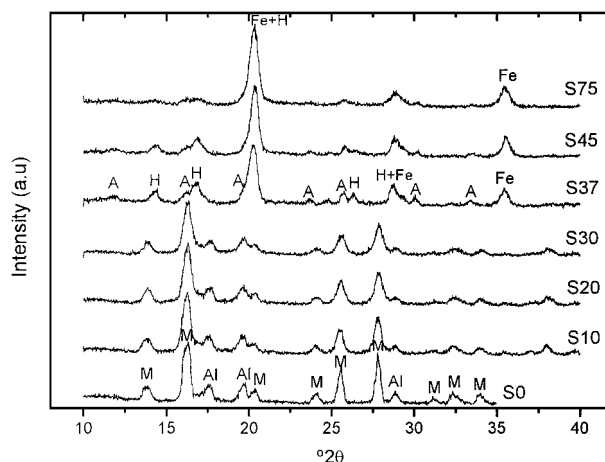


Figure 1 X-ray diffraction patterns of the series of activated samples  $S_0$ – $S_{75}$ . M = magnetite; Al = aluminum; H = hercynite; A = alumina; Fe = iron.

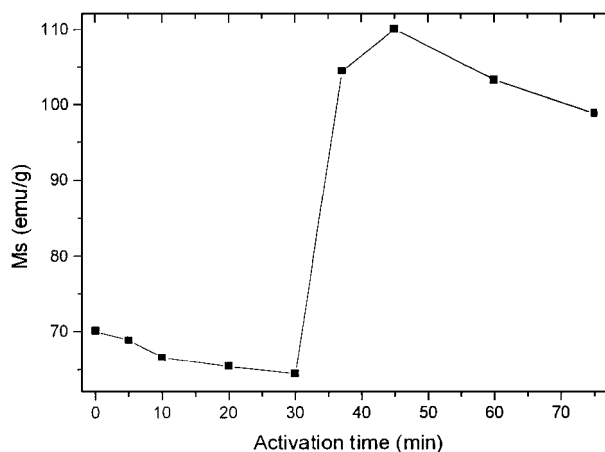


Figure 2 Saturation magnetization  $M_s$  as a function of activation or milling time  $t$  for the series  $S_m$ . The solid line is drawn only as a guide.

and refinement of crystallite size). For  $S_{75}$ , the material consists of small Fe crystallites in an amorphous matrix with some highly deformed  $\text{Al}_2\text{O}_3$  and  $\text{FeAl}_2\text{O}_4$  crystallites.

The values of saturation magnetization  $M_s$  and coercivity  $H_c$  for the series  $S_0$  to  $S_{75}$  are of the order of those reported in the literature for magnetite activated by ball-milling [21]. Markedly distinct behavior is observed on the samples milled for times shorter than 37 minutes and those that were activated for at least 37 minutes. Up to 30 minutes, a slow decrease of  $M_s$  with milling time can be observed, as a consequence of a progressive deterioration of the crystalline structure of the present phases (Fig. 2). A similar effect has already been reported in other papers [15, 16]. It is also observed in this time range that the coercivity increases, due to the gradual decrease of the crystal size (Fig. 3), while for  $S_{37}$  there is an abrupt decrease in coercivity followed by a rather small increase of this magnitude with milling time. This reduction in  $H_c$  coincides with the appearance of free iron and hercynite.

SEM observations of  $S_0$  and  $S_{30}$  (Fig. 4) revealed the decrease of mean particle size (few microns) of  $\text{Fe}_3\text{O}_4$  and Al particles together with an increasing tendency to form agglomerates (several tens of microns).

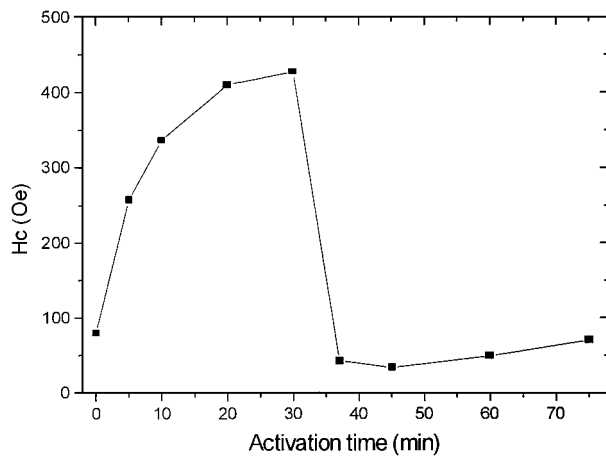
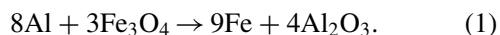


Figure 3 Coercivity  $H_c$  as a function of activation time  $t$  for the series Sm.

Thus, the results obtained from all the used characterization techniques reveal that up to 30 minutes of activation there was not any significant phase transformation.

However, for samples S10, S20 and S30 deposits of metallic Fe were found on the vial walls, indicating that reaction (1) occurred only in some localized points of the system (hot spots) although not extending to the whole reactive mass:



At 37 minutes and beyond, the process of intensive milling induces the ignition of the self-sustained reaction (1) that consumes most of the reactants.

The free Fe that is now present in the powder causes a sudden increase in magnetization (Fig. 2), reaching the highest value in sample S45 (110 emu/g). The features of the reacted system correspond to those of a soft magnetic phase (high  $M_s$  and low  $H_c$ ).

The reduction in saturation magnetization from S45 to S75 is coincident with the gradual decrease of the poorly crystallized hercynite. In this activation time range, some of the formed hercynite is reduced to form free iron and alumina. This fact was supported by Mössbauer spectroscopy measurements [22] and is also consistent with XRD results (Fig. 1). After further milling both hercynite and alumina reduce their crystallinity resulting in lower intensity diffraction peaks and lower magnetization.

### 3.2. Effect of heat treatment

Fig. 5 shows the results of DTA measurements up to 1200°C for samples S0, S10, S30, S37 and S60.

For samples activated up to 37 minutes a complex exothermic band running from 600°C to 700°C is observed. This band is composed of:

(a) an exothermic event at 600°C, noticeable in S0 and S10 and almost indistinguishable in S30. This event corresponds to the oxidation of Al;

(b) an endothermic event at 660°C due to the Al melting;

(c) an exothermic event at 700°C due to reaction (1). After quenching the sample from 750°C the formation of Fe and  $\text{Al}_2\text{O}_3$  is observed in increasing proportion from S10 to S30.

Hercynite only appears after heating up to 1200°C and it may be identified with the wide exothermic band located around 900°C. It can be observed that a low proportion of hercynite is present in S0 and it increases from S0 to S30.

As reaction (1) is triggered during mechanical activation between 30 and 37 minutes, the second exothermic band is not present in samples S37, S45 and S75. (For a detailed discussion of the thermal behavior of Al- $\text{Fe}_3\text{O}_4$  activated mixtures, see reference [23]).

The endothermic event observed in S37, S45 and S75 at approximately 740°C corresponds to the magnetic transformation of the metallic Fe (from ferromagnetic to paramagnetic state) produced during the activation. In sample S60 this effect was observed too, although for the sake of clarity the corresponding DTA curve has not been included in Fig. 4. In the series S0-S30 the magnetic transition is not observed because the Fe produced at 650°C was almost totally transformed to hercynite (as confirmed by XRD). The little amount of heat coming from the small amount of metallic Fe remaining in heat-treated samples S0-S30 might be below the detection limit of the thermal analyzer.

The XRD analyses of samples S0T to S30T (Fig. 6) showed the disappearance of the Al peaks, the formation of hercynite in increasing proportion, and the formation of free iron in low concentration. Magnetite is still present in samples S0T to S10T but it almost disappears in S20T and S30T. This decrease in  $\text{Fe}_3\text{O}_4$  occurs at the same time than the hercynite and iron content is increased.

Comparing S0 with S0T it is possible to observe that Al has reduced part of the magnetite, giving rise to hercynite and iron after the DTA scan.

Sample S37 had already transformed during the mechanochemical treatment, forming hercynite and free Fe. In S37T the content of hercynite increases and also some  $\text{Fe}_2\text{O}_3$  is formed (Fig. 6). S60T and S75T have a higher crystallinity, without formation of any new phases.

Fig. 7 shows the evolution of saturation magnetization as a function of  $t$ , for samples S0T to S75T.

It is remarkable that all  $M_s$  values are considerably lower than any of those obtained for the as-milled samples (Fig. 2). The minimum value (23 emu/g) was attained by S10T, and gradually increased for times longer than 10 minutes.

These  $M_s$  values are abnormally low, since all Fe,  $\text{FeAl}_2\text{O}_4$  and  $\text{Fe}_3\text{O}_4$  have much higher saturation magnetizations. This fact led us to conclude that the iron in these samples should be contained in a phase with lower  $M_s$ , which in the range of sample compositions used, should be of the type  $\text{Fe}[\text{Al}_x\text{Fe}_{2-x}]\text{O}_4$ , with  $0 \leq x \leq 2$ .

The angular position of the diffracted peaks of both hercynite and magnetite as given by PDF (Powder Diffraction Files) are different from those measured in samples SmT. This effect is clearly seen in Fig. 8,

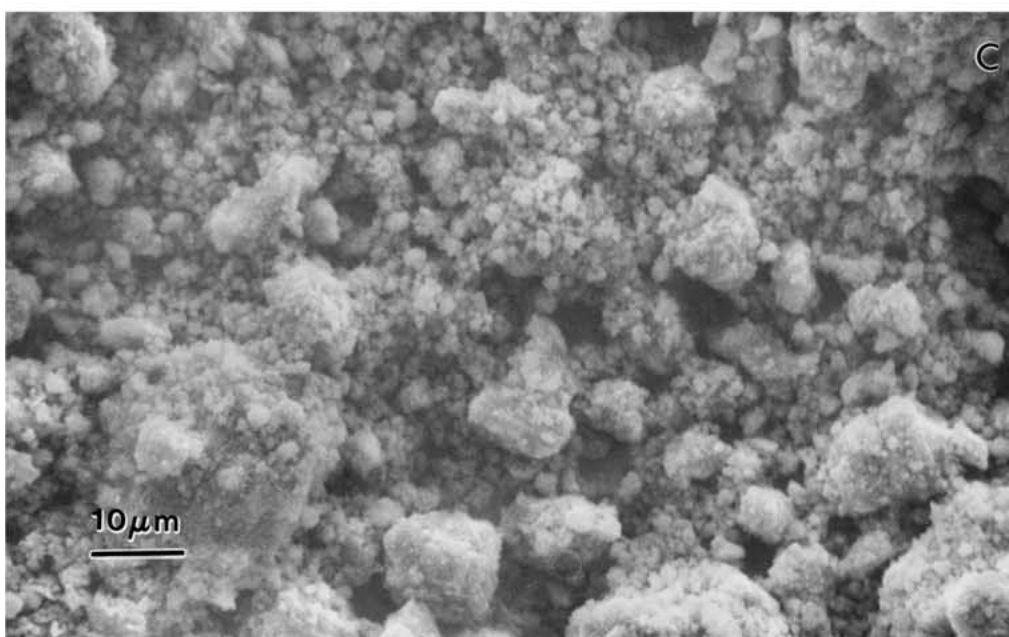
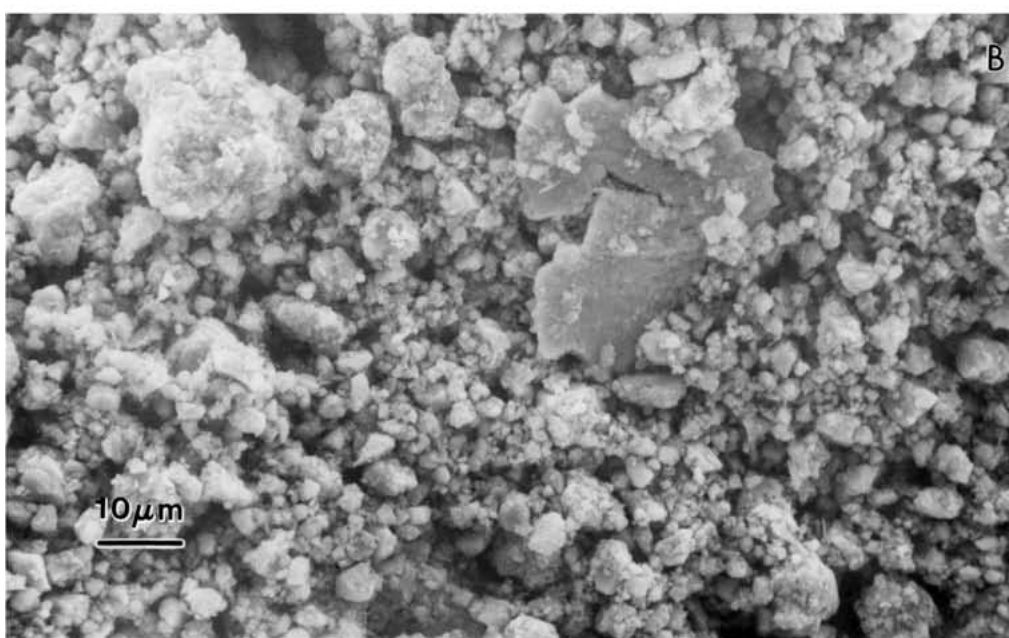
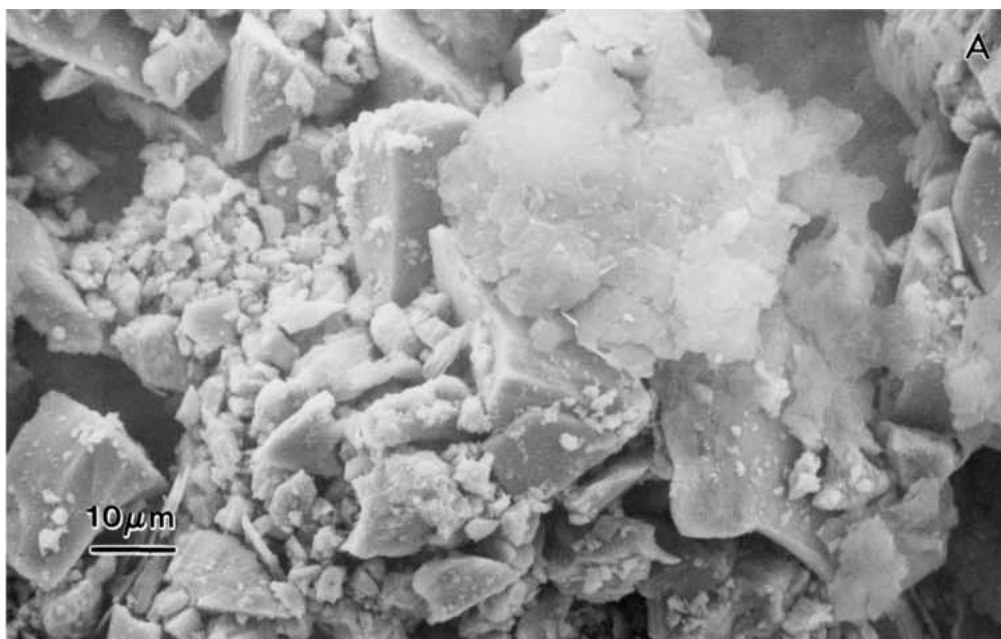


Figure 4 Scanning electron micrographs of samples: (A) S0 (non-activated), (B) S10 and (C) S30.

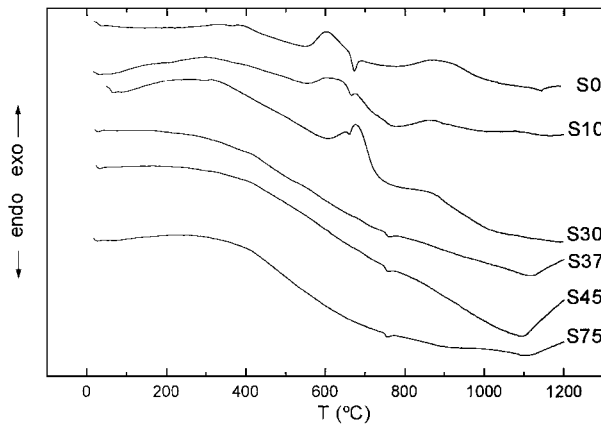


Figure 5 Differential thermal analyses under Ar atmosphere of the series of activated samples.

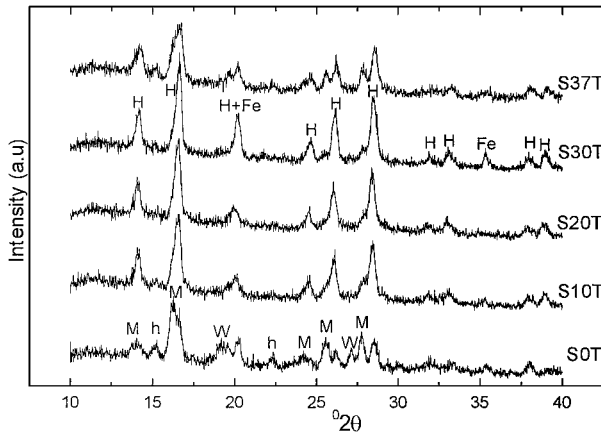


Figure 6 X-ray diffraction patterns of samples S0T to S37T ( $T = 1200^\circ\text{C}$ ). H = hercynite; Fe = iron; M = magnetite; h = hematite; W = wüstite.

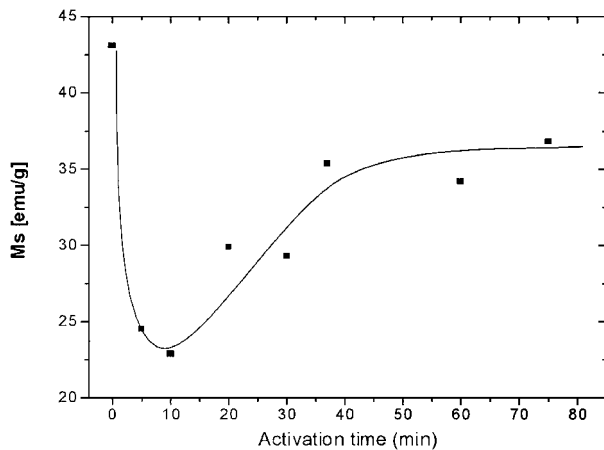


Figure 7 Saturation magnetization  $M_s$  as a function of activation or milling time  $t$  for the series SmT. The solid line is drawn only as a guide.

where the angular position of the (440) diffraction peak is plotted as a function of milling time for the series SmT. The measured values lie in between the hercynite and magnetite PDF values. This supports the view that  $\text{Fe}[\text{Al}_x\text{Fe}_{2-x}]\text{O}_4$  is present in these samples.

The observed changes in the peak position as a function of  $t$  may be accounted for by considering the way in which the transformation occurs. For  $0 \leq t \leq 30$  min hercynite must be formed by diffusion of Al into mag-

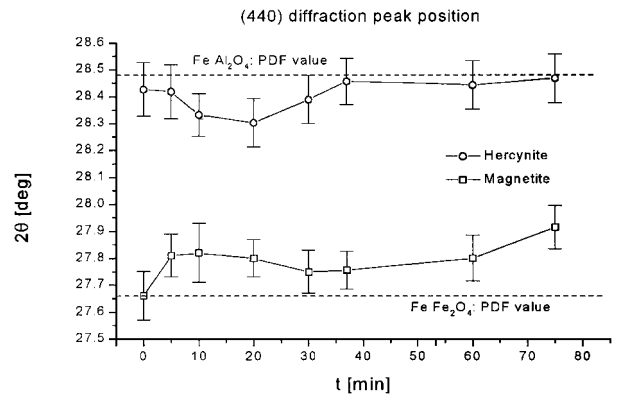


Figure 8 Angular position of the diffraction peak corresponding to planes (440) for hercynite and magnetite, using  $\text{Mo K}\alpha$  radiation. The PDF values for both phases are marked with a dashed line. The solid line is drawn only as a guide.

netite. For increasing milling time, the mean grain size of the particles decreases while the number of defects increases and the diffusion of Al increases with  $t$ , resulting in magnetite with some Al (presumably  $x \sim 0.3$ ) and hercynite with an excess of Fe (presumably  $x \sim 1.5$ ).

For  $t \geq 37$  min hercynite ( $x \sim 2$ ) has already formed during the milling and during the heat treatment some Al diffuses into magnetite shifting the corresponding diffraction peak position to higher values, as the Al content increases with  $t$ .

In such a structure,  $\text{Al}^{3+}$  ions gradually replace the  $\text{Fe}^{3+}$  ions [24, 25]. When  $0 \leq x < 1$  the structure should be that of an inverted spinel, while for  $1 < x \leq 2$  a normal spinel should form. Maximum magnetization occurs for  $x = 0$  and  $x = 2$  while the minimum is for  $x = 1$ . For  $x = 0$  (magnetite),  $M_s$  corresponds to  $4 \mu_B$  per formula unit, giving a resultant  $M_s$  value of 92 emu/g. When  $x = 1$  ( $\text{Fe}[\text{Al Fe}]\text{O}_4$ ), the  $\text{Al}^{3+}$  replace the octahedral  $\text{Fe}^{3+}$ , giving a net magnetization of  $1 \mu_B$  per formula unit. This corresponds to 27 emu/g, close to the value of 23 emu/g observed for S10T.

To our knowledge, no measurements of  $M_s$  and lattice parameter as functions of the  $x$ -value have been made so far.

If we assume that Vegard's law is followed, we need a large amount of hercynite with  $x = 1$  in order to explain the low  $M_s$  value. This should reveal as showing a (440) diffraction peak at  $2\theta \approx 28.08^\circ$ , mid-way between PDF values for magnetite and hercynite. However, the observed value is much higher than this, suggesting that the  $x$ -value is closer to 1.5.

Another way of accounting for this low  $M_s$  value is to consider the modified magnetic interactions due to the presence of  $\text{Al}^{3+}$  ions in the structure. The net effect would be to lower the number of Bohr magnetons per atom and also to produce some canting in the alignment of  $\text{Fe}^{2+}$  and  $\text{Fe}^{3+}$  [24], causing a further decrease in  $M_s$ .

These two points of view are the subject of further work on the studied system.

#### 4. Conclusions

- The mechanochemical activation of  $\text{Al-Fe}_3\text{O}_4$  mixtures produced different effects on the material depending on the milling time:

1. Up to 30 minutes, only structural damage and a reduction of mean crystallite size (reaching about 12 nm for Fe<sub>3</sub>O<sub>4</sub>) was observed. A material of relatively low  $M_s$  (64.5 emu/g) and relatively high  $H_c$  (427 Oe) was obtained.

2. At 37 minutes the exothermic self-sustained reaction (1) occurred in most of the sample, yielding metallic Fe and Al<sub>2</sub>O<sub>3</sub> and afterwards hercynite is formed. The produced material had a high  $M_s$  (110 emu/g) and low  $H_c$  (34 Oe). The best combination  $M_s$ - $H_c$  was obtained for the sample activated for 45 minutes

3. For times longer than 37 minutes the system gradually evolves through the partial reduction of FeAl<sub>2</sub>O<sub>4</sub> to Fe and Al<sub>2</sub>O<sub>3</sub>. The final structure of the material consists on crystals of Fe immersed into a low-crystallinity matrix with some Al<sub>2</sub>O<sub>3</sub> and FeAl<sub>2</sub>O<sub>4</sub>.

- Thermal treatments up to 1200°C under Ar atmosphere of activated samples produced the following effects:

1. The mixtures activated during 30 minutes or less (barely reacted) underwent reaction (1) at about 700°C.

2. The values of saturation magnetization measured for SmT are considerably lower than those of Sm. This is presumably due to the gradual replacement of Al<sup>3+</sup> for Fe<sup>3+</sup> in the octahedral sites of hercynite which leads to the formation of a variable composition spinel phase Fe [Al<sub>x</sub> Fe<sub>2-x</sub>] O<sub>4</sub> with  $0 \leq x \leq 2$ .

3. S10T attains the lowest  $M_s$  value. This may be ascribed to the presence of Fe [Al Fe] O<sub>4</sub> ( $x = 1$ ) since this composition corresponds to the minimum possible magnetization attainable in the spinel phase or to canting in the magnetic ions due to the dilution effects of Al ions in the spinel structure.

## Acknowledgments

The authors wish to thank CONICET, CIC, UNMdP, Agencia Córdoba Ciencia and SECyT-UNC the financial support given for the realization of this work.

## References

1. P. MATTEAZZI, G. LE CAËR and A. MOCELLIN, *Ceram. Int.* **23** (1997) 39.
2. E. GAFFET, F. BERNARD, J.-C. NIEPCE, F. CHARLOT, C. GRAS, G. LE CAËR, J.-L. GUICHARD, P. DELCROIX, A. MOCELLIN and O. TILLEMENT, *J. Mater. Chem.* **9** (1999) 305.
3. D. GARCÍA, S. SCHICKER, J. BRUHN, R. JANSSEN and N. CLAUSSEN, *J. Amer. Ceram. Soc.* **80**(9) (1997) 2248.
4. C. KUHRT and L. SCHULTZ, *J. Appl. Phys.* **71**(4) (1992) 1896.
5. P. MILLET and T. HWANG, *J. Mater. Sci.* **31** (1996) 351.
6. R. REN, Z. YANG and L. L. SHAW, *Nanostruct. Mater.* **11**(1) (1999) 25.
7. A. MAITRE and P. LEFORT, *Solid State Ionics* **104** (1997) 109.
8. E. MA, J. PAGÁN, G. CRANFORD and M. ATZMON, *J. Mater. Res.* **8**(8) (1993) 1836.
9. J. Z. JIANG, L. GERWARD and S. MØRUP, *J. Metas. Nanocrys. Mater.* **2-6** (1999) 115.
10. V. SEPELÁK, S. WIßMANN and K. D. BECKER, *J. Mater. Sci.* **33** (1998) 2845.
11. C. GÓMEZ-YÁÑEZ, C. BENÍTEZ and H. BALMORIRAMÍREZ, *Ceramics International* **26**(3) (2000) 271.
12. D. OSSO, O. TILLEMENT, G. LECAËR and A. MOCELLIN, *Proc. 8th World Ceramic Congress (CIMTEC'94)*, edited by P. Vincenzini (Faenza Editrice, 1994).
13. N. J. WELHAM, T. KERR and P. E. WILLIS, *J. Amer. Ceram. Soc.* **82**(9) (1999) 2332.
14. L. TAKACS and M. PARDAVI-HORVATH, *J. Appl. Phys.* **73**(10) (1993) 6958.
15. P. G. BERCOFF and H. R. BERTORELLO, *J. Mag. Magn. Mat.* **187** (1998) 169.
16. *Idem.*, *ibid.* **205** (1999) 261.
17. L. TAKACS, *Materials Letters* **13** (1992) 119.
18. J. L. GUICHARD, O. TILLEMENT and A. MOCELLIN, *J. Mater. Sci.* **32** (1997) 4513.
19. L. TAKACS and M. PARDAVI-HORVATH, *J. Appl. Phys.* **75**(10) (1994) 5864.
20. P. M. BOTTA, E. F. AGLIETTI and J. M. PORTO LÓPEZ, *Mater. Chem. Phys.*, in press.
21. E. PETROVSKÝ, M. D. ALCALÁ, J. M. CRIADO, T. GRYGAR, A. KAPICKA and J. SUBRT, *J. Mag. Magn. Mat.* **210** (2000) 257.
22. P. M. BOTTA, R. C. MERCADER, E. F. AGLIETTI and J. M. PORTO LÓPEZ, unpublished results.
23. P. M. BOTTA, E. F. AGLIETTI and J. M. PORTO LÓPEZ, *Termochim. Acta* **363** (2000) 143.
24. J. SMIT and H. P. WIJN, "Ferrites" (John Wiley & Sons, New York, 1959).
25. O. ALEJOS, C. DE FRANCISCO, J. M. MUÑOZ, P. HERNÁNDEZ, C. TORRES, J. I. ÍÑIGUEZ and L. TORRES, *J. Mag. Magn. Mat.* **202** (1999) 141.

Received 2 February 2001

and accepted 24 January 2002